

Striped gold nanoparticles: New insights from molecular dynamics simulations

Cite as: J. Chem. Phys. **144**, 244710 (2016); <https://doi.org/10.1063/1.4954980>

Submitted: 05 April 2016 . Accepted: 17 June 2016 . Published Online: 30 June 2016

 Vasumathi Velachi, Debdeep Bhandary, Jayant K. Singh, M. Natália D. S. Cordeiro, et al.



View Online



Export Citation



CrossMark

ARTICLES YOU MAY BE INTERESTED IN

[Comparison of simple potential functions for simulating liquid water](#)

The Journal of Chemical Physics **79**, 926 (1983); <https://doi.org/10.1063/1.445869>

[A coarse-grain molecular dynamics study of oil-water interfaces in the presence of silica nanoparticles and nonionic surfactants](#)

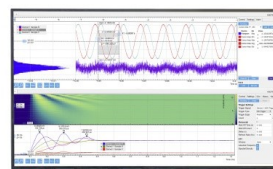
The Journal of Chemical Physics **146**, 204702 (2017); <https://doi.org/10.1063/1.4984073>

[Thermal transport at a nanoparticle-water interface: A molecular dynamics and continuum modeling study](#)

The Journal of Chemical Physics **150**, 114701 (2019); <https://doi.org/10.1063/1.5084234>

Challenge us.

What are your needs for
periodic signal detection?



Zurich
Instruments

Striped gold nanoparticles: New insights from molecular dynamics simulations

Vasumathi Velachi,^{1,a)} Debdip Bhandary,² Jayant K. Singh,²
and M. Natália D. S. Cordeiro^{1,b)}

¹LAQV@REQUIMTE/Department of Chemistry and Biochemistry, University of Porto,
4169-007 Porto, Portugal

²Department of Chemical Engineering, Indian Institute of Technology Kanpur, Kanpur 208016, India

(Received 5 April 2016; accepted 17 June 2016; published online 30 June 2016)

Recent simulations have improved our knowledge of the molecular-level structure and hydration properties of mixed self-assembled monolayers (SAMs) with equal and unequal alkyl thiols at three different arrangements, namely, random, patchy, and Janus. In our previous work [V. Vasumathi *et al.*, *J. Phys. Chem. C* **119**, 3199–3209 (2015)], we showed that the bending of longer thiols over shorter ones clearly depends on the thiols' arrangements and chemical nature of their terminal groups. In addition, such a thiol bending revealed to have a strong impact on the structural and hydration properties of SAMs coated on gold nanoparticles (AuNPs). In this paper, we extend our previous atomistic simulation study to investigate the bending of longer thiols by increasing the stripe thickness of mixed SAMs of equal and unequal lengths coated on AuNPs. We study also the effect of stripe thickness on the structural morphology and hydration of the coated SAMs. Our results show that the structural and hydration properties of SAMs are affected by the stripe thickness for mixtures of alkyl thiols with unequal chain length but not for equal length. Hence, the stability of the stripe configuration depends on the alkyl's chain length, the length difference between the thiol mixtures, and solvent properties. *Published by AIP Publishing.* [<http://dx.doi.org/10.1063/1.4954980>]

I. INTRODUCTION

Gold nanoparticles' (AuNPs) properties can be fine-tuned by grafting ligands onto them such that the physicochemical properties of their surfaces are controlled by the structure and chemistry of the anchored ligands.^{1,2} Further, these ligands serve as linkers between the AuNPs and the environment and provide a range of interesting properties to the materials, for example, solubility, stability, and electrochemical charging.^{1,3–7} Due to the unique properties of monolayer coated AuNPs, a powerful class of materials have emerged for a wide variety of applications, ranging from sensing to catalysis, including drug delivery, electron transfer efficiency, electrochemical charging, and molecular recognition.^{1,8–13} Significant work has been focused on the development of monolayer-protected AuNPs, e.g., improving the biocompatibility of AuNPs, inhibiting AuNPs aggregation, and preventing protein adsorption. Furthermore, monolayer-protected AuNPs enhance favorable interactions with biological membranes.^{14–18} However, the referred properties of monolayer-protected AuNPs can be achieved more efficiently by grafting multiple ligand species to the NP surface. Indeed, mixed-ligand monolayer coated AuNPs boost the preferential interactions between the specific ligands and their surroundings. For example, the surface charge density of AuNPs can be adapted by coating with a mixture of charged and uncharged ligands.^{19–21} Besides, the mixing of thiols may

lead to a microphase separation of the two ligand species—forming a Janus pattern, or to a completely mixed phase of the ligands—forming randomly or patchy/striped patterns.²² It is apparent that the organization of the ligands can affect also the overall behavior of NPs. Janus particles preserve the individual ligand properties, thus possessing bifunctional properties that have been used in many applications.²³ Random arrangements instead tend to display the average properties of each ligand molecule. Meanwhile, stripe/patchy arrangements of ligands give structure-dependent properties such as interfacial energy and solubility that make them attractive in potential applications, for instance, in protein inhibition, catalysis, and molecular recognition.^{24–27} Experimental studies have confirmed the possibility of the three structural morphologies of AuNPs coated with aromatic and aliphatic compounds, namely, random, patchy/stripe, and Janus particles.²² In a recent paper,²⁸ we have studied and compared the structural and hydration properties of mixed self-assembled monolayers (SAMs) with equal and unequal carbon chains on AuNPs at three different arrangements. We have observed that the organization of thiol mixtures affects the hydration of the SAMs as well as the structural properties of SAMs.²⁸ Among the three nanoscale morphologies (i.e., Janus, random, and stripe/patchy), the striped morphology can have significant consequences for particle behavior, as the striped particles were shown to non-disruptively penetrate into cells whereas similar particles with other morphologies were unable to penetrate.^{29,30} Over the last decade or so, a series of papers have been published by Stellacci and co-workers^{31–34} on striped nanoparticles, these being probed by various

^{a)}vasuphy@gmail.com

^{b)}ncordeir@fc.up.pt

experimental methods. Moreover using numerical simulations, Singh *et al.*³⁵ showed that the formation of stripes is due to the entropic gains and the length mismatch between the ligands. Later on, Ghorai and Glotzer³⁶ investigate also through numerical simulations which are the model parameters that control the stripe thickness on 7 nm size AuNPs. The authors showed that the stripe thickness might depend on parameters like the head group's charges, the relative length difference of the tails, and the strength of repulsions. However, the effect of the above parameters on the structural properties of stripe pattern is lacking. Indeed, though past studies have focused on the understanding of the formation of the stripe morphology on NPs and controlling parameters, the microscopic picture of such morphology is still unclear. Nonetheless the latter is crucial for a better design and handling of nanomaterials in a biological environment. To the best of our knowledge, no previous simulation work has yet been carried to address the effect of stripe thickness on the microscopic structural and hydration properties of striped AuNPs.

In this work, we carried out a detailed atomistic simulation study of mixed monolayer protected AuNPs with various stripe thicknesses. The monolayer consists of a binary mixture of thiols with longer and shorter lengths. For comparison purposes, we also performed the simulation of mixed SAMs of thiols with equal lengths. The rest of the paper is organized as follows: in Sec. II, we give details of the systems as well as of the applied simulation conditions; the results from our MD simulations are then presented and discussed in Section III, and finally, in Section IV, the main summary and conclusions of this study are given.

II. SIMULATION DETAILS

In this work, an all atom representation is employed to model the AuNPs coated with alkanethiols. Using Material studio 6.0,³⁷ we built up icosahedral AuNPs with a diameter of 4 nm, containing 1985 Au atoms. These icosahedral AuNPs have multiple facets such as {111} and {100} but the overall structure looks almost spherical. Thus, the alkanethiols were grafted radially away from the AuNPs with a distance between the sulfur atoms and AuNPs surface of 2.38 Å with the surface density of ~ 14 Å²/molecule. The striped morphology with various thicknesses was defined by AuNPs coated with

alternating lines containing one/two/three/four of each ligand species. Since we aim to study the hydration and structural properties of SAMs at various stripe thicknesses, the gold and sulfur atoms were fixed throughout the simulations. In our recent study,²⁸ we found that the structural and hydration properties were constant for mixed thiols with C5 length coated on 4.0 nm AuNPs at three different arrangements and differ for those with C11 length. Particularly, the results from the number of water molecules within the SAMs radius lead us to conclude that the thiols coated on 4.0 nm size AuNPs with C5 length are almost similar to those of thiols coated on non-curved surfaces. Therefore, we believe that the stripe thickness may not affect the AuNPs coated with thiols of C5 carbon chain lengths. Here, we considered hydrophobic and hydrophilic thiols with C11 carbons [S(CH₂)₁₁CH₃ and S(CH₂)₁₁COOH] and mixtures of hydrophobic thiols with C5 carbons and hydrophilic thiols with C11 carbons [S(CH₂)₅CH₃ and S(CH₂)₁₁COOH] and vice versa [S(CH₂)₁₁CH₃ and S(CH₂)₅COOH] at the four different stripe thicknesses. From now on, the above mixing will be denoted as C11–C11COOH, C5–C11COOH, and C11–C5COOH, respectively. Initial structures in Figs. 1–3 depict the surface morphologies at the four stripe thicknesses considered in this work, which in turn will be hereafter denoted as 1-sam, 2-sam, 3-sam, and 4-sam, respectively. Note that it is likely that a single stripe morphology would be thermodynamically preferred based on the ligand properties, but here, we assume that any given arrangement is possible. To investigate the effect of length difference of thiols on the 1-sam stripe morphology, we considered also the following mixings: C2/CnCOOH–Cn/C2COOH (where n = 4, 5, 6, and 7), C5–C8COOH/C9COOH, and C7–C10COOH/C11COOH. We have considered 1:1 mixture composition for all the cases.

To compare the effect of stripe thickness on the structure and hydration properties of mixed SAMs with unequal chains on curved surfaces with those on non-curved surfaces, we simulated also mixed SAMs of C5/C11–C11COOH/C5COOH coating the Au (111) surface. The latter was modeled using six atomic layers, each layer comprising 1728 atoms with lateral dimensions of 119.63×103.61 Å² ($x = 119.63$ Å and $y = 103.61$ Å). Based on experimental results,³⁸ the alkanethiols are bounded to the surface through the S atom

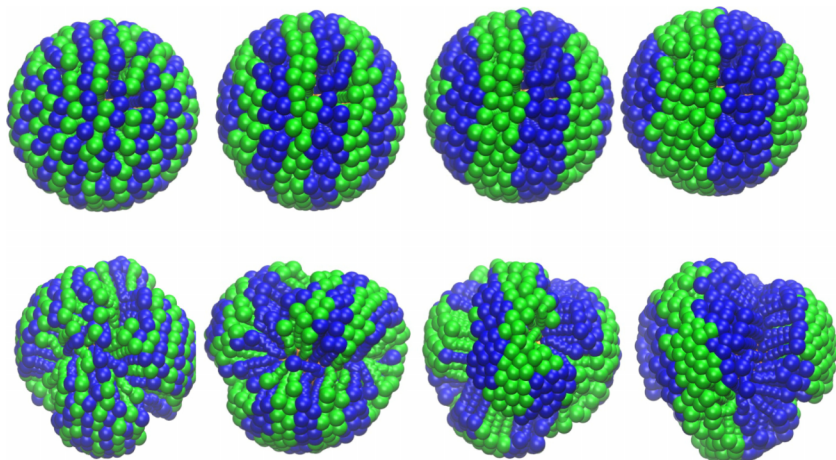


FIG. 1. Snapshots of initial (top row) and equilibrated (bottom row) structures of the AuNPs coated with mixed SAMs of C11–C11COOH at various stripe thicknesses, namely: 1-sam, 2-sam, 3-sam, and 4-sam (from left to right). Blue (methyl terminated alkanethiols) spheres and green (carboxyl terminated alkanethiols) spheres represent the two species of SAMs.

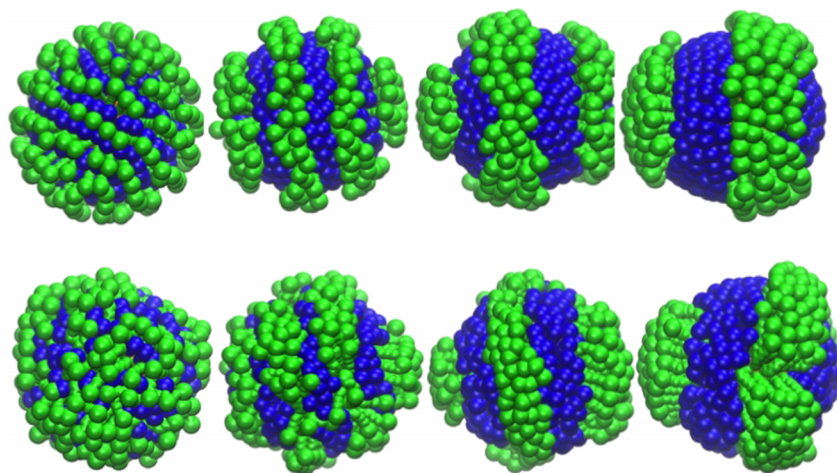


FIG. 2. Snapshots of initial (top row) and equilibrated (bottom row) structures of the AuNPs coated with mixed SAMs of C5–C11COOH at various stripe thicknesses, namely: 1-sam, 2-sam, 3-sam, and 4-sam (from left to right). Color coding as in Fig. 1.

on-top binding-sites and form a densely ($\sim 21.6 \text{ \AA}^2/\text{molecule}$) packed layer arranged into a $(\sqrt{3} \times \sqrt{3})R30^\circ$ lattice. Finally, all the coated AuNPs were solvated with a sufficient number of water molecules (ca. 67 100) by placing the coated AuNPs at the center of a cubic box of dimensions of about $140 \times 140 \times 140 \text{ \AA}^3$. In the case of coated Au(111) surfaces, the latter were kept at the bottom of the simulation box and then a water droplet of $\sim 9 \text{ nm}$ (19 993 molecules) was added above the SAM surface. Periodic boundary conditions were applied in all Cartesian directions for AuNPs. However, for the case of coated surfaces, periodic boundary conditions were applied only in the xy plane parallel to the surface. In doing so, a water liquid/vapor interface is created along the z direction. Thus, a reflecting wall was placed in the xy plane at just above the water droplet to prevent evaporation of the water molecules and to maintain a fixed vapor pressure. The all-atom intermolecular interactions for SAMs were described by the CHARMM27³⁹ force field that has already been successfully applied in MD simulations of SAMs on gold surface in previous studies.^{28,40–43} The interactions between gold atoms⁴⁴ of the NPs and those between gold and sulfur atoms were modeled by the Lennard–Jones (LJ) intermolecular potential. Standard Lorentz–Berthelot⁴⁵ combining rules were

applied for calculating the LJ cross-interaction parameters. Harmonic bond stretching, angle bending, and dihedral angle terms were taken from the CHARMM27 force field.

All MD simulations were performed using the LAMMPS package.⁴⁶ The AuNPs system simulations were performed in the NpT ensemble and the gold surface-droplet simulations in the NVT ensemble. The Verlet leapfrog algorithm⁴⁷ was used to integrate the equations of motion, with a time step of 1.0 fs. The temperature was kept constant at 298 K and the pressure at 1 atm by means of the Nosé–Hoover thermostat coupled with the Parrinello–Rahman barostat^{48,49} with a relaxation constant of 0.1 ps. The Particle–Particle Particle–Mesh (PPPM) method⁵⁰ was used to handle the long-range electrostatic interactions with the real-space cutoff distance set to 12 \AA and the error tolerance to 10^{-5} . The short-range LJ interactions were smoothly shifted to zero between 10 and 12 \AA . The SHAKE algorithm⁵¹ was applied to constraints of the bonds in water molecules. All the analyses described in this paper were carried out by averaging over the last 2 ns of 4–5 ns MD-trajectories. The VMD software⁵² was employed to visualize the trajectories and collecting the snapshots.

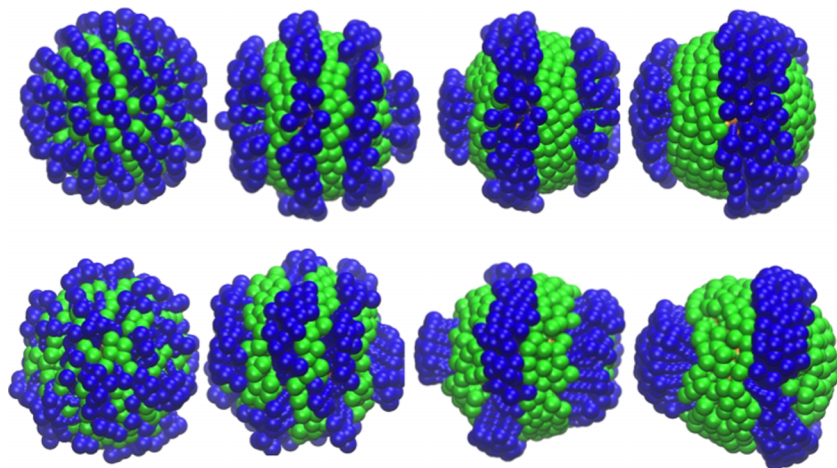


FIG. 3. Snapshots of initial (top row) and equilibrated (bottom row) structures of the AuNPs coated with mixed SAMs of C11–C5COOH at various stripe thicknesses, namely: 1-sam, 2-sam, 3-sam, and 4-sam (from left to right). Color coding as in Fig. 1.

III. RESULTS AND DISCUSSION

A. Comparison of AuNPs coated with mixed SAMs of lowest ($\Delta l = 0$) and largest ($\Delta l = 6$) length difference

Let us first look at the snapshots of the equilibrium structures from the atomistic simulations of C11–C11COOH, C5–C11COOH, and C11–C5COOH mixed SAMs on AuNPs at various stripe thicknesses (see Figs. 1–3). These snapshots show how the nature of stripe configurations changes upon the change in stripe thickness for thiols mixtures with equal and unequal length. As can be seen, in the case of equal-length mixtures, there is no significant variation on the stripe configurations at the various thicknesses, though a somewhat division is observed for the methyl terminated stripe domain at higher stripe thicknesses. It is known that longer thiol coating on curved surfaces leads to thiols segregation to maintain the terminal groups distance at ~ 5 Å.^{28,53} Therefore, due to the phase segregation of carboxyl terminated thiols, the methyl terminated thiols are divided and tend to set apart nearby carboxyl terminated clusters for higher stripe thicknesses (3-sam and 4-sam). While in the case of mixtures with unequal chain length, the snapshots show noticeable changes on the stripe configurations by changing the stripe thickness. At lower stripe thicknesses (1-sam and 2-sam), the longer thiols do not have the next nearest longer thiols for cohesive interactions between hydrocarbon chains. That causes the longer thiols to bend over shorter ones, leading to a collapse of the stripe configuration. The stripe configuration is however stable for 3-sam and 4-sam stripe thicknesses. Before we move on, however, it is useful to analyze the position density of C5 and C11 carbon atoms that will give a clearer microscopic picture of the stripe arrangements rather than the qualitative one provided by the snapshots. In Figs. 4–6, we present the average position density of

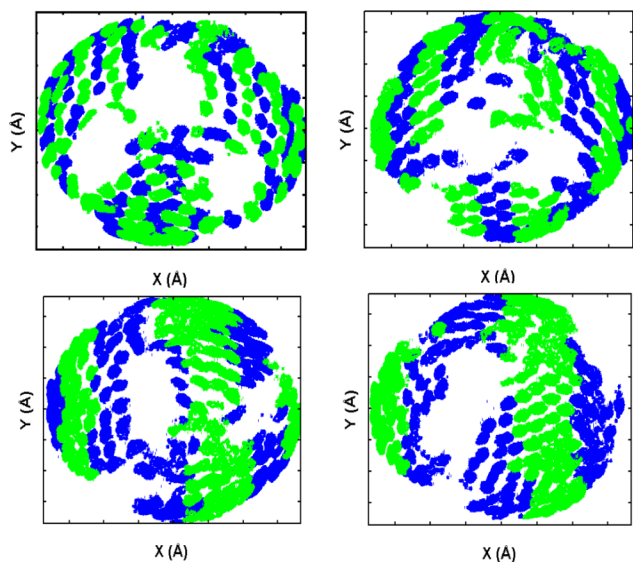


FIG. 4. Density distributions of C11 carbon atoms from upper half of C11–C11COOH mixed SAMs coated AuNPs that are projected into the xy plane at four kinds of stripe thicknesses: 1-sam (upper left), 2-sam (upper right), 3-sam (lower left), and 4-sam (lower right). The methyl terminated carbons and carboxyl terminated carbons are shown by blue and green colors, respectively.

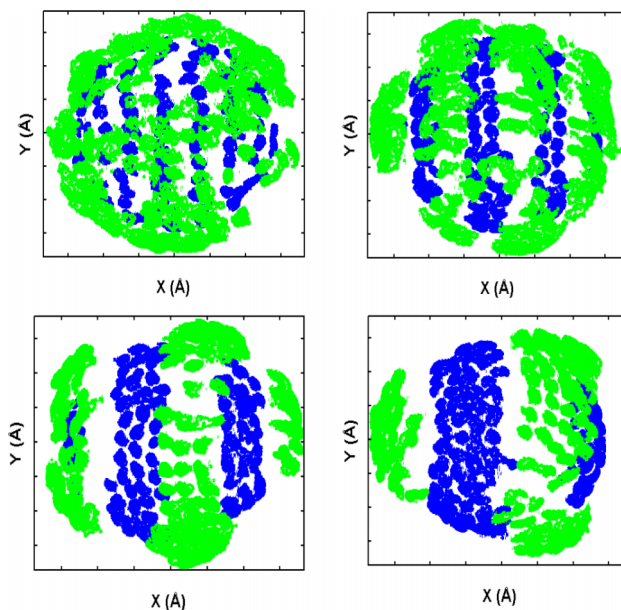


FIG. 5. Density distributions of C5 and C11 carbon atoms from upper half of C5–C11COOH mixed SAMs coated AuNPs that are projected in the xy plane at four kinds of stripe thicknesses: 1-sam (upper left), 2-sam (upper right), 3-sam (lower left), and 4-sam (lower right). Color coding as in Fig. 4.

C11 and C5 carbon atoms calculated from the upper half coated AuNPs and then projected into the xy plane. Notice that overlapping of the densities of carbon atoms associated with the terminal groups of thiols indicates a collapse of the stripe arrangement, whereas distinctly separated carbon densities provide evidence of stable stripe configurations. In the case of C11–C11COOH mixing (Fig. 4), although the thiols form groups, the stripe arrangement appears to be persisting in all the cases. On the opposite, in the case of mixing of unequal lengths at lower stripe thicknesses, one can see that the stripe arrangement collapses for longer thiols (see Figs. 5 and 6). Furthermore, some of the shorter thiols are seen

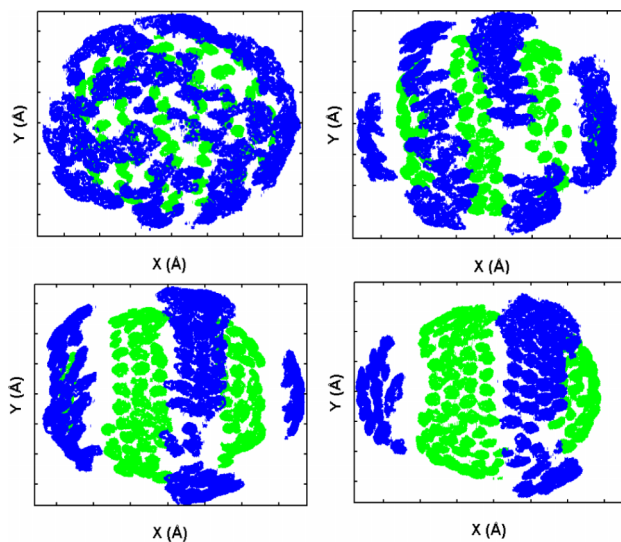


FIG. 6. Density distributions of C11 and C5 carbon atoms from upper half of C11–C5COOH mixed SAMs coated on AuNPs that are projected into the xy plane at four kinds of stripe thicknesses: 1-sam (upper left), 2-sam (upper right), 3-sam (lower left), and 4-sam (lower right). Color as coding in Fig. 4.

to be hidden by the longer thiols, which in turn provide an indication about the accessibility of the shorter thiols binding sites for biomolecules and other molecules that are used in potential applications. That is, at lower stripe thicknesses, the interactions of shorter thiols with foreign molecules will be hindered by the longer thiols. However for the higher stripe thicknesses, one can observe clear phase separated densities, and hence, shorter thiols do have binding accessibility towards foreign molecules.

B. Bending of thiols

Generally, longer thiols tend to bend over the shorter ones when there is a sufficient relative length difference between them since that imparts greater flexibility.^{28,34} To investigate the possibility of such a bending in the various striped patterns, we have calculated the end-to-end distance (R) of the longer thiols that affords a measurement of their bending. Fig. 7 shows the probability distributions of R/R_0 , $P(R/R_0)$, for C5–C11COOH and C11–C5COOH mixing at various stripe thicknesses, where R being the end-to-end distance, i.e., the distance between the C1 and C11 carbon atoms, and R_0 the geometric length of the carbon chain. The two distinct peaks observed at $R/R_0 = 1$ and at $R/R_0 < 1$ correspond to thiols without bending and with bending, respectively. At lower stripe thicknesses, owing to the lack of cohesive interactions between the hydrocarbon chains of longer thiols, these bend over the shorter ones. As seen, AuNPs with 1-sam and 2-sam striped patterns show higher probability of bending, whereas a less bending is observed for thicker stripes. Among these 1-sam and 2-sam striped patterns, 1-sam shows the maximum bending. In addition, due to the force of attraction between water molecules and the carboxyl terminal groups, the probability of bending is higher for C5–C11COOH mixing compared to the bending observed for the C11–C5COOH mixtures. The next step is to probe the

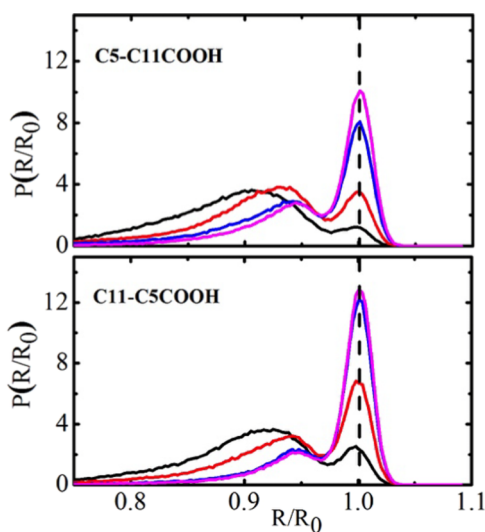


FIG. 7. Probability distributions of the end-to-end (C1 to C11) distance for C5–C11COOH and C11–C5COOH mixing at four kinds of stripe thicknesses, namely: 1-sam (black color), 2-sam (red color), 3-sam (blue color), and 4-sam (pink color).

effect of stripe thickness on other structural parameters of the SAMs.

C. Radius of gyration and tilt angles

To infer the conformational changes of adsorbed thiols with the stripe thickness, we have examined the size of the SAMs coated AuNPs by computing their radius of gyration (R_g) for the four stripe thicknesses (Table I). The R_g values of C11–C11COOH are higher when compared to those of SAMs of mixed thiols with unequal lengths, just as we have reported for diverse coating arrangements in our earlier study.²⁸ From Table I, one can clearly notice that the size of the SAM-coated AuNPs does not change with respect to the stripe thickness for C11–C11COOH but it varies for unequal-length mixtures. Indeed in the latter, the unequal length of chains favors bending of longer thiols over the shorter thiols, and hence, the sizes of coated AuNPs are smaller. However, thinner stripes allow higher bending of longer thiols over shorter ones, and thus, the R_g values of thinner stripes (1-sam and 2-sam) are lower than those of the corresponding thicker stripes (3-sam and 4-sam). That is, the R_g values increase as the stripe thickness increases for mixing of thiols with unequal lengths. The observed difference in the probability of bending of longer thiols among the C5–C11COOH and C11–C5COOH mixtures follows however an opposite trend to that displayed by the R_g values (Table I), since these are slightly higher for C11–C5COOH than for C5–C11COOH.

Another important structural property to judge the effect of the stripe thickness is the tilt angle of alkanethiols when adsorbed on the NP surface. The tilt angle of thiols coated on AuNPs can be calculated by finding the angle between the vector joining the sulfur head-group and the odd carbons of the alkyl chain and the vector perpendicular to the surface of the sphere and passing through the sulfur head-group.^{38,53} The calculated tilt angles for all cases are presented in Table II. In accordance with the independency of the size of the coated AuNPs with the stripe thickness for C11–C11COOH mixing, here also, the average tilt angles (30 ± 13 , 31 ± 14 , 29 ± 13 , and 31 ± 12) from both kinds of thiols follow the same independency. However, the average tilt angles corresponding to the individual types of thiols show variations with respect to the stripe thickness. At lower stripe thicknesses, the phase segregation is more widespread, and thus, the tilt angles do not show variations among the methyl and carboxyl terminated thiols. Whereas, in the case of thicker stripes, due to the hydrogen bonding interactions between the carboxyl groups, the carboxyl-terminated groups are phase segregated and that lowers their tilt angles. For mixing of thiols with unequal lengths, longer thiols exhibit

TABLE I. Radius of gyration (\AA) for the AuNPs coated with mixed SAMs for all the studied cases.

CH ₃ –COOH	1-sam	2-sam	3-sam	4-sam
C11–C11	28.52 ± 0.90	28.47 ± 0.90	28.53 ± 0.90	28.40 ± 0.90
C5–C11	26.82 ± 0.85	26.90 ± 0.85	27.12 ± 0.86	27.20 ± 0.86
C11–C5	26.84 ± 0.85	27.02 ± 0.86	27.25 ± 0.86	27.26 ± 0.86

TABLE II. Average tilt angle (degree) of the mixed SAMs for all the studied cases.

CH ₃ -COOH	1-sam		2-sam		3-sam		4-sam	
	CH ₃	COOH						
C11-C11	30 ± 13	30 ± 13	31 ± 14	31 ± 14	31 ± 13	28 ± 13	36 ± 12	26 ± 12
C5-C11	21 ± 11	36 ± 14	21 ± 12	36 ± 13	22 ± 12	32 ± 14	22 ± 12	29 ± 12
C11-C5	35 ± 14	19 ± 11	31 ± 14	20 ± 11	28 ± 14	22 ± 11	25 ± 12	23 ± 12

larger tilt angles than the ones corresponding to shorter thiols, which goes in line with previous computational results.^{28,36} That is, the tilt angle normally increases by increasing the carbon chain length for a fixed NP, just as our tilt angles for unequal-length mixtures do reveal. In fact, the probability of bending of longer thiols decreases with increasing stripe thickness, which essentially leads to a decrease in the average tilt angles. When comparing the tilt angle of longer thiols in the C5-C11COOH and C11-C5COOH SAMs, those with carboxyl terminal groups show higher tilt angles than the other ones. Due to the strong attractive forces between water and the COOH groups that bring water molecules closer to C5COOH in the C11-C5COOH SAM, thus, its longer thiols have lesser space for tilting. However, in the case of the C5-C11COOH SAM, there are no such attractive forces between the shorter thiols and water, and thus, the carboxyl terminated longer thiols display higher tilt angles. On the other hand, as a result of the longer thiol bending and the strong interactions between water and the COOH terminated shorter thiols, the dynamics of the latter are restrained, and hence, their tilt angles are lower for C11-C5COOH at thinner stripes. Our results from the structural properties of SAMs clearly reveal that the stripe thickness has impact on the structural properties of SAMs. The next question to be addressed is then what will be the effect of the stripe thickness on the hydration properties of SAMs?

D. Hydration of SAMs and hydrogen bonds

To investigate the effect of stripe thicknesses on the hydration of SAMs, we have calculated the number of water molecules (N_w) nearby the SAMs. Our recent study²⁸ has shown that the major changes in the N_w values are observed only within the radius of SAMs, and thus, we present here the N_w values within such a radius, excluding the terminal groups (Table III). In the case of unequal-length mixtures, the radius of the SAMs was calculated by considering the longer thiols. From Table III, we can see that the number of water molecules is independent of the stripe thickness for C11-C11COOH mixing. Interestingly, a strong dependency of the number

of water molecules on the stripe thickness is observed for unequal-length mixing. Since the interaction strength of water molecules with carboxyl groups is much stronger than with methyl groups, a large number of water molecules are found near to shorter thiols for the C11-C5COOH mixing than for the C5-C11COOH mixing. At lower stripe thicknesses, the bended longer thiols with higher tilting cause steric hindrance to the water molecules that are approaching towards the shorter thiols, resulting in lower N_w values. Though the number of water molecules within the radius of SAMs gives information about the binding ability of shorter thiols towards foreign molecules, the hydrogen bonds between the carboxyl groups and waters will give a clearer picture to that ability. Hence, we have calculated the hydrogen bonds between the latter by adopting the criterion prescribed by Luzar and Chandler.⁵⁴ According to this criterion, a hydrogen bond exists if the distance between the participating oxygen atoms is less than 3.5 Å and simultaneously the O-H...O angle is less than 30°. The calculated values of number of hydrogen bonds per carboxyl group (N_{CO-w}) are summarized in Table IV. As one can infer from Table IV, for all kinds of mixing, the N_{CO-w} values vary with the stripe thickness. In the case of C11-C11COOH mixing, the N_{CO-w} value decreases as the stripe thickness increases, which is found to be true also for C5-C11COOH. However, an opposite trend is found in the case of C11-C5COOH mixing. For instance, at thinner stripes, the C11-C5COOH mixture shows lower values of N_{CO-w} due to the presence of shorter thiols with carboxyl terminal groups and the longer thiol bending over these. In the case of C11-C11COOH and C5-C11COOH mixings, the increase in the stripe thickness allows some inter-carboxyl hydrogen bonding that leads to a disruption of some of the water-carboxyl hydrogen bonding (see Table V). Because of the length mismatch in C5-C11COOH, the longer carboxyl-terminated thiols display more orientational freedom to form hydrogen bonds with waters, and hence, the N_{CO-w} values are slightly larger than those appearing in C11-C11 mixing. From the results pertaining to the density of carbon atoms and longer thiol bending, we hypothesize that the binding nature of thiols with other molecules in striped AuNPs is

TABLE III. Average number of water molecules (N_w) within the radius of SAMs (excluding terminal groups).

CH ₃ -COOH	1-sam	2-sam	3-sam	4-sam
C11-C11	479 ± 20	462 ± 22	480 ± 26	411 ± 24
C5-C11	286 ± 30	403 ± 48	858 ± 36	1076 ± 36
C11-C5	488 ± 33	824 ± 31	1237 ± 32	1339 ± 40

TABLE IV. Average number of water-carboxyl terminal group hydrogen bond (N_{CO-w}) per carboxyl terminal group.

CH ₃ -COOH	1-sam	2-sam	3-sam	4-sam
C11-C11	2.25 ± 0.08	2.19 ± 0.08	2.16 ± 0.08	2.11 ± 0.07
C5-C11	2.32 ± 0.08	2.35 ± 0.08	2.23 ± 0.08	2.13 ± 0.08
C11-C5	1.92 ± 0.07	2.01 ± 0.07	2.06 ± 0.07	2.10 ± 0.07

TABLE V. Average total number of carboxyl-carboxyl hydrogen bonds ($N_{\text{CO-CO}}$) in the mixed SAMs.

$\text{CH}_3\text{-COOH}$	1-sam	2-sam	3-sam	4-sam
C11-C11	2.92 ± 0.63	6.61 ± 0.96	7.26 ± 1.40	9.13 ± 0.46
C5-C11	9.10 ± 0.94	6.41 ± 0.71	7.94 ± 1.18	11.21 ± 0.63
C11-C5	7.56 ± 1.04	9.26 ± 1.10	11.73 ± 1.57	12.04 ± 1.14

affected by the stripe thickness. These results confirm that the hydration of SAMs depends on the structural arrangement of thiols. It should be noticed here that, in close agreement to these results, the experimental studies^{25,26} observed that the ligand shell morphology affects the solubility of the AuNPs almost as much as the molecular composition. Finally, our results shed insight into the effect of stripe thickness on the structural and hydration properties of SAMs. Particularly, the stripe arrangement was found to collapse for unequal-length mixtures at the lowest thickness (1-sam). Ghorai and Glotzer³⁶ reported that the length of thiols and the length mismatch are one of the factors affecting the stripe thickness on 7 nm size AuNPs. Such findings prompted us to the question: What could be the relative length difference and length of the thiols with which the stripe configuration is stable at 1-sam stripe thickness? We address such a question in Sec. III E.

E. AuNPs coated with mixed SAMs of varying length difference ($\Delta l = 2, 3, 4, 5$)

To investigate the difference in the chain lengths with which the stripe pattern is stable at the lowest stripe thickness, we have considered a length difference between the thiols ranging from two to five CH_2 groups, i.e., we tackled the following mixed SAMs: $\text{C}_2\text{-C}_n\text{COOH}$ and $\text{C}_n\text{-C}_2\text{COOH}$, where $n = 4, 5, 6,$ and 7 . The probability distribution of longer thiols bending and the average position densities of C_2 and C_n carbon atoms for all the cases are shown in Figs. 8–10.

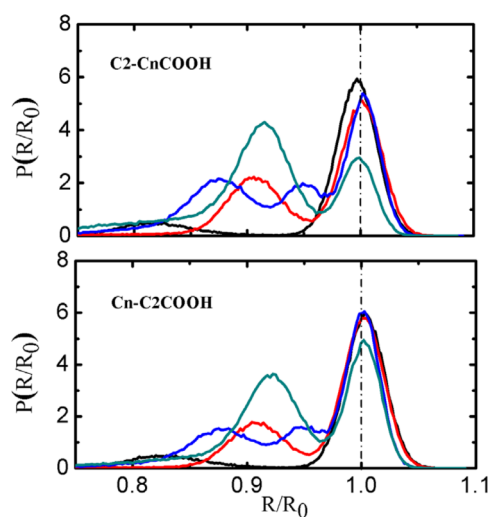


FIG. 8. Probability distributions of the end-to-end (C1 to C_n) distance for $\text{C}_2\text{-C}_n\text{COOH}$ and $\text{C}_n\text{-C}_2\text{COOH}$ (where $n = 4, 5, 6,$ and 7) mixing at 1-sam stripe thickness with four kinds of relative length differences, namely: $\Delta l = 2$ (black color), $\Delta l = 3$ (red color), $\Delta l = 4$ (blue color), and $\Delta l = 5$ (cyan color).

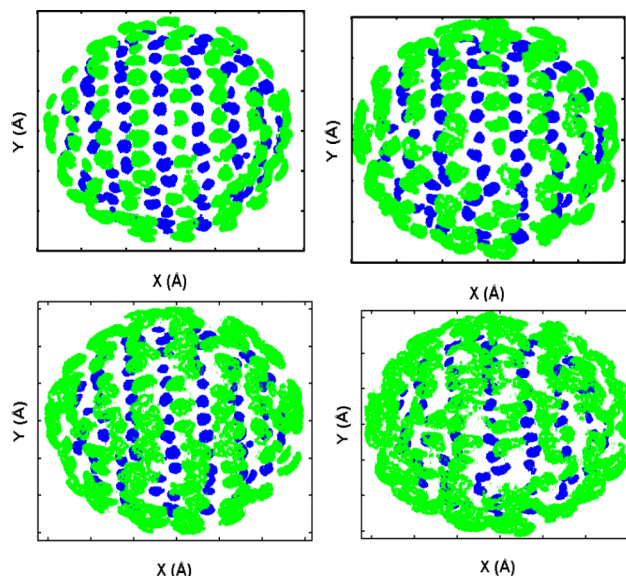


FIG. 9. Density distribution of C_2 and C_n carbon atoms from upper half of $\text{C}_2\text{-C}_n\text{COOH}$ mixed SAMs coated on AuNPs that are projected in xy plane at four kinds of relative length differences, namely: $\Delta l = 2$ (upper left), $\Delta l = 3$ (upper right), $\Delta l = 4$ (lower left) and $\Delta l = 5$ (lower right). Color coding: methyl terminated carbons (C_2)—blue, and carboxyl terminated carbons (C_n)—green.

As seen in these figures, the observed maximum probability of bending and the overlapping between the densities of C_2 and C_n carbon atoms reveals that a relative length difference of $\Delta l = 2\text{-}4$ (two-three CH_2 groups) for the thiols shows a stable stripe pattern but that of $\Delta l = 5$ reveals a collapse of stripe pattern. The monolayer formation of thiols with C_5 length on 4 nm AuNPs shows almost a similar kind of packing of thiols on a non-curved surface.²⁸ That is, thiols

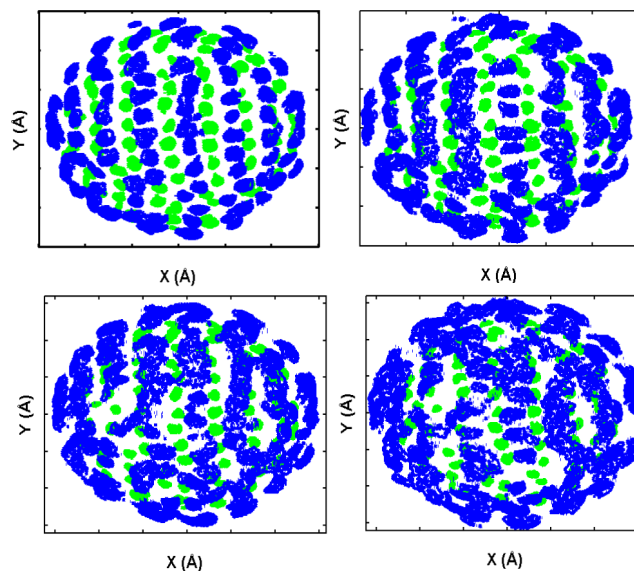


FIG. 10. Density distribution of C_n and C_2 carbon atoms from upper half of $\text{C}_n\text{-C}_2\text{COOH}$ mixed SAMs coated on AuNPs that are projected into the xy plane at four kinds of relative length differences, namely: $\Delta l = 2$ (upper left), $\Delta l = 3$ (upper right), $\Delta l = 4$ (lower left), and $\Delta l = 5$ (lower right). Color coding: methyl terminated carbons (C_n)—blue, and carboxyl terminated carbons (C_2)—green.

with above five CH_2 groups have its own free volume along with the free volume provided by the shorter thiols that give adequate flexibility for bending and tilting. Therefore, mixed SAMs of thiols with a relative length difference of five CH_2 groups undergo collapse of stripes but not below this. Let us now check the nature of the stripe configuration for the relative length difference of thiols at three-four CH_2 groups by increasing their length. We investigate that by simulating mixed SAMs of two types, namely, (i) C5–C n ($n = 8, 9$), and (ii) C7–C m ($m = 10, 11$). We analyzed that the longer thiol bending probability distributions as well as the densities of carbon atoms and the obtained results are presented in Figs. 11 and 12. The corresponding end-to-end probability distributions of the two SAMs are shown in Fig. 11. For both the cases, four CH_2 groups favor collapse of stripes, indicated by the higher probability at $R/R_0 < 1$, whereas three CH_2 shows some intermittent behavior with higher probability at $R/R_0 = 1$. This demonstrates that the persistence of stripe configuration at 1-sam stripe thickness depends on the length of thiols as well as on their relative length difference. So far, we have discussed the effect of stripe thickness on the structural and hydration properties of SAMs coated on AuNPs. Thereafter, the interesting question is what will be the effect of stripe thickness on the properties of SAMs coated on a non-curved gold surface? Particularly, will it be a similar kind of effect or a different one? In Sec. III F, we will discuss the results obtained for the mixed SAMs coating the gold(111) surface at the four different stripe thicknesses.

F. Au(111) surface coated with mixed SAMs

Our results on the effect of stripe thickness for equal-length SAM mixtures coating the AuNPs do not show differences in their properties. Further, longer thiol bending

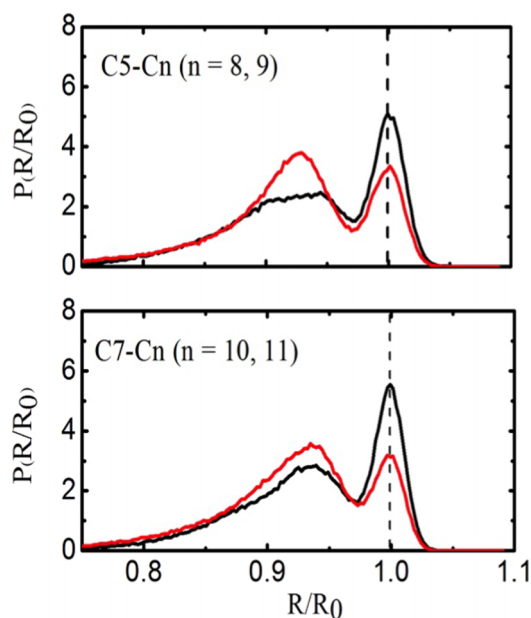


FIG. 11. Probability distributions of the end-to-end (C5/C7 to C n /C m) distance for C5/C7–C n COOH/C m COOH (where $n = 8$ and 9 ; $m = 10$ and 11) mixing at 1-sam stripe thickness with two kinds of relative length differences, namely: $\Delta l = 3$ (black color) and $\Delta l = 4$ (red color).

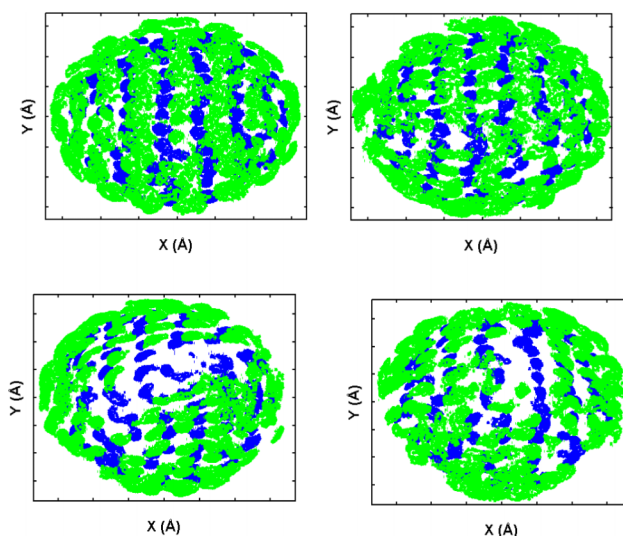


FIG. 12. Density distribution of C5/C7 and C n /C m carbon atoms from upper half of mixed SAMs (upper row refers to C5–C8COOH/C9COOH and bottom row refers to C7–C10COOH/C11COOH) coated on AuNPs that are projected into the xy plane at two kinds of relative length differences. $\Delta l = 3$ (left column) and $\Delta l = 4$ (right column). Color coding: methyl terminated carbons (C n)—blue, and carboxyl terminated carbons (C2)—green.

caused the major changes in the structure and hydration properties of SAMs at various stripe thicknesses. Moreover, our recent study²⁸ on mixed SAMs with equal lengths grafting a gold surface at three different arrangements revealed almost the same surface hydrophobicity and a slight variation in the thickness of SAMs. Hence, we believe that there will be no effect on the properties of SAMs upon change in the stripe thickness for mixing of thiols with equal lengths on non-curved surfaces. Thus, we present here the results of the Au(111) surface coated with mixed SAMs of unequal lengths such as C5–C11COOH and C11–C5COOH. Figs. 13–15 depict the bending of longer thiols and the one-dimensional density

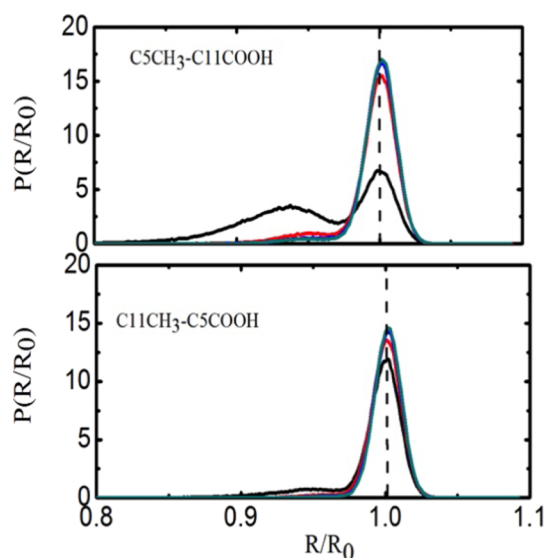


FIG. 13. Probability distributions of the end-to-end (C1 to C11) distance for C5–C11COOH and C11–C5COOH mixing at four kinds of stripe thicknesses, namely: 1-sam (black color), 2-sam (red color), 3-sam (blue color), and 4-sam (cyan color).

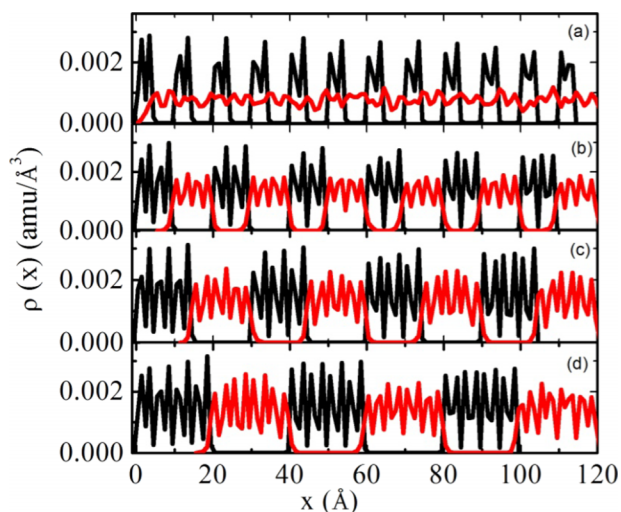


FIG. 14. Mass density profile of carbon atoms along the stripe direction (x axis) of C5–C11COOH mixed SAMs coated on Au surface at four kinds of stripe thickness. (a) 1-sam, (b) 2-sam, (c) 3-sam, and (d) 4-sam. Color coding: C5 carbon atom—black color, and C11 carbon atom—red color.

of carbon atoms. The maximum probability of bending is observed only for C5–C11COOH at 1-sam stripe thickness (Fig. 13(a)) with a smaller peak at $R/R_0 < 1$ whereas for other stripe thicknesses, there is no such peak and thus a negligible bending probability. In Figs. 14 and 15, the two clear separated distinct crests and cliffs appearing in the density profiles of carbon atoms of shorter and longer thiols indicate a stable stripe configuration. In other words, the minimum and maximum densities of the carbon atoms of longer thiols should not overlap in the shorter thiols region for stable stripe configurations. In the case of 1-sam stripe thickness for C5–C11COOH mixing (Fig. 14(a)), it does not show zero density for the longer thiols at the shorter thiols region, implying longer thiol bending and thus the collapse of the stripe configuration. In contrast, as regards the C11–C5COOH mixing (Fig. 15(a)), it does not show longer thiol bending and overlapping densities, and hence, a stable stripe configuration is observed. However, we found a slight change in the hydration of SAMs for 1-sam stripe thickness compared with the other stripe thicknesses. The reason behind such a small change is due to the less available free space

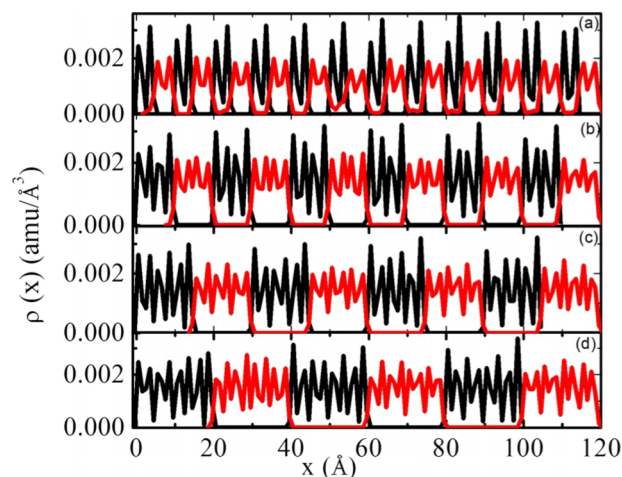


FIG. 15. Mass density profile of carbon atoms along the stripe direction (x axis) of C11–C5COOH mixed SAMs coated on Au surface at four kinds of stripe thickness. (a) 1-sam, (b) 2-sam, (c) 3-sam, and (d) 4-sam. Color coding: C5 carbon atom—black color, and C11 carbon atom—red color.

(5 Å) provided by the shorter thiols for water molecules in comparison to the other cases (10 Å, 15 Å, and 20 Å). Besides, the C5–C11COOH mixing shows major changes on the hydration of SAMs upon changes in the stripe thickness. Our results are in line with the computational results obtained by Centrone *et al.*,²⁵ pertaining to the wetting behavior on surfaces with different ordering patterns, using ethanol as solvent. Indeed these authors reported that the solubility of the gold surface coated with phase-separated mixtures of ligands depends critically on the ordering pattern of the ligand shell. We hypothesize that the observed stable stripe configuration for C11–C5COOH at 1-sam is due to the occupancy of water molecules in the free volume provided by the shorter thiols, which is determined by the difference in water liking and hating nature of the terminal groups. To test our hypothesis, we have simulated the C11–C5COOH mixture on the gold surface at vacuum with 1-sam stripe thickness and have analyzed the longer thiol bending as well as the one dimensional carbon densities (see Fig. 16). The observed probability of longer thiol bending and overlapping densities confirms that the longer thiols bend over the shorter ones when there are no water molecules, while no such a bending is seen for the wetted

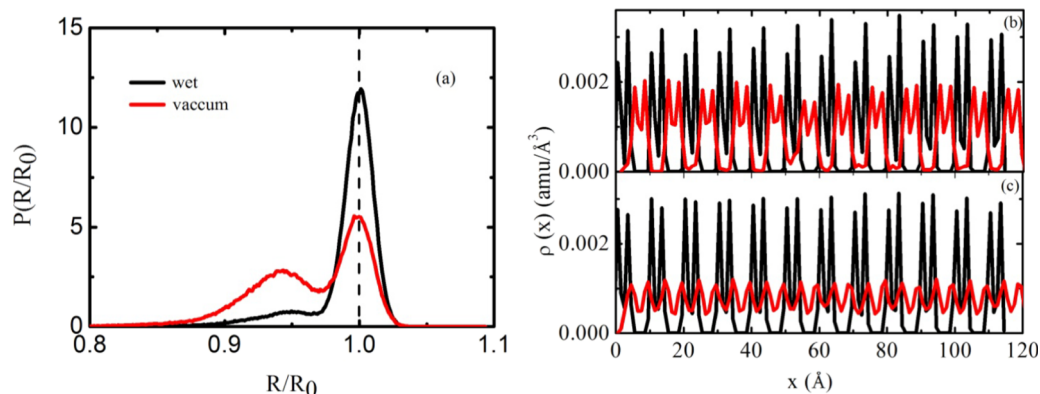


FIG. 16. Probability distribution of end-to-end distance (a), and mass density profile of carbon atoms along the stripe direction for C11–C5COOH mixed SAMs coated on Au surface at wetting (b) and vacuum (c). Color coding in (b) and (c): C5 carbon atom—black color, and C11 carbon atom—red color.

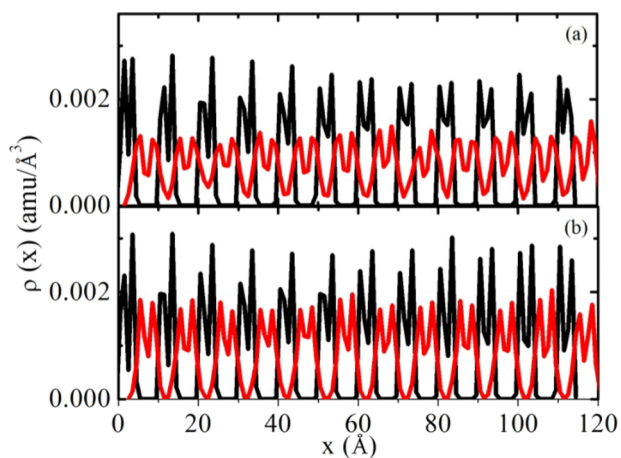


FIG. 17. Mass density profile of carbon atoms along the stripe direction of mixed SAMs coated on Au surface at 1-sam stripe thickness. (a) C5-C10COOH and (b) C5-C9COOH. Color coding: C5 carbon atom—black color, and C10/9 carbon atom—red color.

SAMs. Inspection of these results leads us to conclude that the stability of the stripe configuration also depends on the size of the solvent molecules and the interaction strength of these with the terminal groups of thiols. Additional simulations on the C5-C10COOH and C5-C9COOH mixtures (five CH₂ and four CH₂ groups) coating the Au surface demonstrate that the stability of stripe configuration depends on the relative SAMs length difference (Fig. 17). In particular, we predict that a stable stripe configuration occurs on flat surfaces if the relative difference is \leq four CH₂ groups and above that, the stripe configuration gets collapsed. Hence, our results suggest that even on flat surfaces, the stability of the stripe configuration at 1-sam stripe thickness depends on the length mismatch but not on the length of thiols *per se*.

G. Non-bonded energetic background

Ghorai and Glotzer³⁶ showed that electrostatic interactions between the tail groups play a role in the stripe formation by considering tail groups with positive and negative charges in their simulation. In the present study, the SAM tail groups are neither positively nor negatively charged but do have hydrophobic or hydrophilic character. Due to the presence of different electron affinity of heavy atoms in the hydrophobic (C) and hydrophilic (C, O) tail groups, the interaction energy between the methyl and carboxyl tail groups will differ from those within the same groups. Since there is no chance of chemical bonding between the methyl and carboxyl groups during monolayers formation, we therefore only take into account the interaction energies coming from non-bonded interaction contributions, i.e., the sum of electrostatic and van der Waals interactions. To compare the effect of stripe thickness on the interaction energies among the equal-length and unequal-length mixtures, we consider the following mixed SAMs on AuNPs: C11-C11COOH, C5-C11COOH, and C11-C5COOH. The calculated values are given in Table VI. As seen, for all the cases, the interaction energy between the methyl and carboxyl tail groups for 1-sam stripe thickness is greater than that for the other stripe thicknesses. As the

TABLE VI. Non-bonded interaction energy (kcal/mol) between methyl and carboxyl terminal groups.

CH ₃ -COOH	1-sam	2-sam	3-sam	4-sam
C11-C11	-93.14 ± 3.55	-55.42 ± 2.87	-37.38 ± 2.61	-29.93 ± 2.10
C5-C11	-47.03 ± 2.80	-32.21 ± 2.52	-17.57 ± 1.82	-8.73 ± 1.44
C11-C5	-35.61 ± 2.61	-16.36 ± 2.10	-6.23 ± 1.00	-2.87 ± 0.68

stripe thickness increases, the methyl and carboxyl tail groups are more distorted leading to a decrease in the interaction energy. In the case of C11-C11COOH, the observed greater interaction energy between the methyl and carboxyl tail groups for 1-sam stripe thickness suggests that stronger interaction energies produce a stable stripe pattern. However, for the unequal-length mixture cases show contrary to the above, i.e., greater interaction energy between the methyl and carboxyl tail groups for 1-sam stripe thickness may not give a perfect stripe pattern; instead, it gives collapsed stripe pattern. That is, these energetic results suggest that a stronger interaction energy may lead to striped AuNPs for all the cases, even though a stable stripe pattern was achieved only for equal-length mixtures and not for unequal-length ones. To test the hypothesis of a possible correlation between the interaction energy and the stable stripe pattern for the case of unequal-length mixing, we calculated the interaction energy between the tail groups for the C11-C5COOH mixed SAM at 1-sam stripe thickness on the gold surface in wet condition and as well as in vacuum. Using the same method, the interaction energies found were -22.57 ± 1.28 kcal/mol and -73.34 ± 3.82 kcal/mol for wet and vacuum, respectively. Our results of longer thiol bending and carbon densities of the above two cases (see Fig. 16) predicted that the stable stripe pattern was observed for wet surface and not for vacuum, which implies greater (-73.34 ± 3.82 kcal/mol) interaction energy between methyl and carboxyl may not provide perfect stripe pattern for unequal-length mixtures. This thus led us to conclude that one cannot decide the stability of the stripe pattern from the interaction energy between the tail groups in the case of thiols with unequal-length mixing. In addition, our results show that the interaction energy between the tail groups depends on the stripe thickness, the length of the thiols, and the solvent properties.

IV. SUMMARY AND CONCLUSIONS

In this work, we have carried out all-atom MD simulations of mixed SAMs on a gold spherical NP and a flat surface to investigate the effect of stripe thickness on the structural and hydration properties of SAMs. These simulations enabled us to probe how the stripe thickness affects such properties for SAMs of mixed thiols with equal and unequal carbon lengths. For example, structural properties such as the tilt angle and *R_g* values show dependency on the stripe thickness for unequal-length thiol mixtures. Our results on longer thiol bending probability distributions and densities of carbon atoms reveal that the stripe configuration collapses at lower stripe thickness but persists for higher stripe thickness. Further, we find that

the stability of stripe configuration on AuNPs at lower stripe thickness depends on the relative length difference between the thiols and their lengths as well. That is, the relative length difference varies with respect to the length of the thiols for inducing the stable stripe configuration on coated AuNPs. However, for the gold flat surface, a stable stripe configuration is observed when the thiol's length difference is \leq four CH₂ groups collapsing above that. In fact, our results pertaining to the flat surface reveal that the stability of the SAM's stripe configuration not only depends on the relative lengths but it also depends on the chemical composition of the terminal groups and solvent. Particularly, the results from stripped C11–C5COOH SAMs on Au surface at water and vacuum led us to conclude that the stability of the stripe configuration depends on the solvent's size and its interactions with the thiols. Therefore, it should be possible to obtain stable striped configurations by the judicious choice of the solvent and the thiols' terminal groups. A detailed study on the stability of striped AuNPs of various terminal groups at various organic solvents is thus of utmost importance in this field of research. We believe that the present study provides a better understanding of the microscopic picture of the stripe configurations arising from various relative length differences of thiol tails on 4 nm size AuNPs. Our findings have also relevant implications for biological processes. For instance, the findings regarding the hydrogen bonding between water and thiols show the binding nature of the various stripped AuNPs with any other foreign molecules that are used for potential applications.

ACKNOWLEDGMENTS

This work was supported by the European Union (FEDER funds through COMPETE) and National Funds (FCT, Fundação para a Ciência e Tecnologia) through Project No. UID/QUI/50006/2013. The work also received financial support from the Department of Science & Technology, Govt. of India, and Indo-Portugal Collaboration funded by International Division of DST, Government of India (Grant No. INT/PORTUGAL/P-05/2013). The authors thank all financing sources as well as the HPC Centre, IIT Kanpur for computational facility.

¹M. C. Daniel and D. Astruc, *Chem. Rev.* **104**, 293–346 (2004).

²A. Verma and F. Stellacci, *Small* **6**, 12–21 (2009).

³K. G. Thomas and P. V. Kamat, *Acc. Chem. Res.* **36**, 888–898 (2000).

⁴A. N. Shipway, E. Katz, and I. Willner, *ChemPhysChem* **1**, 18–52 (2000).

⁵C. C. You, M. De, G. Han, and V. M. Rotello, *J. Am. Chem. Soc.* **127**, 12873 (2005).

⁶C. E. D. Childsey, *Science* **251**, 919–922 (1991).

⁷T. Gu, J. K. Whitesell, and M. A. Fox, *J. Org. Chem.* **69**, 4075 (2004).

⁸P. Pengo, S. Polizzi, L. Pasquato, and P. Scrimin, *J. Am. Chem. Soc.* **127**, 1616–1617 (2005).

⁹N. L. Rosi and C. A. Mirkin, *Chem. Rev.* **105**, 1547–1562 (2005).

¹⁰P. Ghosh, G. Han, M. De, C. K. Kim, and V. M. Rotello, *Adv. Drug Delivery Rev.* **60**, 1307–1315 (2008).

¹¹M. De, P. S. Ghosh, and V. M. Rotello, *Adv. Mater.* **20**, 4225–4241 (2008).

¹²D. Aili, M. Mager, D. Roche, and M. M. Stevens, *Nano Lett.* **11**, 1401–1405 (2011).

¹³M. Lucarini, P. Franchi, G. F. Pedullini, C. Gentilini, S. Polizzi, P. Pengo, P. Scrimin, and L. Pasquato, *J. Am. Chem. Soc.* **127**, 16384–16385 (2005).

¹⁴T. L. Doane and C. Burda, *Chem. Soc. Rev.* **41**, 2885 (2012).

¹⁵S. Jiang, K. Y. Win, S. Liu, C. P. Teng, Y. Zheng, and M.-Y. Han, *Nanoscale* **5**, 3127–3148 (2013).

¹⁶C.-C. You, M. De, and V. M. Rotello, *Curr. Opin. Chem. Biol.* **9**, 639–646 (2005).

¹⁷A. E. Nel, L. Mädler, D. Velegol, T. Xia, E. M. V. Hoek, P. Somasundaran, F. Klaessig, V. Castranova, and M. Thompson, *Nat. Mater.* **8**, 543–557 (2009).

¹⁸D. F. Moyano and V. M. Rotello, *Langmuir* **27**, 10376–10385 (2011).

¹⁹J. Simard, C. Briggs, A. K. Boal, and V. M. Rotello, *Chem. Commun.* **2000**, 1943–1944.

²⁰O. Uzun, Y. Hu, A. Verma, S. Chen, A. Centrone, and F. Stellacci, *Chem. Commun.* **2008**, 196–198.

²¹S. Kubowicz, J. Dailant, M. Dubois, M. Delsanti, J.-M. Verbavatz, and H. Möhwald, *Langmuir* **26**, 1642–1648 (2010).

²²X. Liu, M. Yu, H. Kim, M. Mameli, and F. Stellacci, *Nat. Commun.* **3**, 1182 (2012).

²³S. Jiang, Q. Chen, M. Tripathy, E. Luijten, K. S. Schweizer, and S. Granick, *Adv. Mater.* **22**, 1060–1071 (2010).

²⁴J. J. Kuna, K. Voitchovsky, C. Singh, H. Jiang, S. Mwenifumbo, P. K. Ghorai, M. M. Stevens, S. C. Glotzer, and F. Stellacci, *Nat. Mater.* **8**, 837–842 (2009).

²⁵A. Centrone, E. Penzo, M. Sharma, J. W. Myerson, M. Jackson, N. Marzari, and F. Stellacci, *Proc. Natl. Acad. Sci. U. S. A.* **105**, 9886–9891 (2008).

²⁶A. Ghosh, S. Basak, B. H. Wunsh, R. Kumar, and F. Stellacci, *Angew. Chem., Int. Ed.* **50**, 7900–7905 (2011).

²⁷X. Liu, Y. Hu, and F. Stellacci, *Small* **7**, 1961–1966 (2011).

²⁸V. Vasumathi, D. Bhandary, J. K. Singh, and M. N. D. S. Cordeiro, *J. Phys. Chem. C* **119**, 3199–3209 (2015).

²⁹A. Verma, O. Uzun, Y. Hu, Y. Hu, H. S. Han, N. Watson, S. Chen, D. J. Irvine, and F. Stellacci, *Nat. Mater.* **7**, 588–595 (2008).

³⁰R. P. Carney, T. M. Carney, M. Mueller, and F. Stellacci, *Biointerphases* **7**, 17 (2012).

³¹A. M. Jackson, J. W. Myerson, and F. Stellacci, *Nat. Mater.* **3**, 330–336 (2004).

³²A. M. Jackson, Y. Hu, P. J. Silva, and F. Stellacci, *J. Am. Chem. Soc.* **128**, 11135–11149 (2006).

³³Q. K. Ong, J. Reguera, P. J. Silva, M. Moglianetti, K. Harkness, M. Longobardi, K. S. Mali, C. Renner, S. D. Feyter, and F. Stellacci, *ACS Nano* **7**, 8529–8539 (2013).

³⁴E. S. Cho, J. Kim, B. Tejerina, T. M. Hermans, H. Jiang, H. Nakanishi, Y. Miao, A. Z. Patashinski, S. C. Glotzer, F. Stellacci, and B. A. Grzybowski, *Nat. Mater.* **11**, 978–985 (2012).

³⁵C. Singh, P. K. Ghorai, M. A. Horsch, A. M. Jackson, R. G. Larson, F. Stellacci, and S. C. Glotzer, *Phys. Rev. Lett.* **99**, 226106 (2007).

³⁶P. K. Ghorai and S. C. Glotzer, *J. Phys. Chem. C* **114**, 19182–19187 (2010).

³⁷Material Studio Modeling Environment, Release 6, Accelrys Software, Inc., San Diego, CA, USA, 2011.

³⁸M. C. Vargas, P. Giannozz, A. Selloni, and G. Scoles, *J. Phys. Chem. B* **105**, 9509–9513 (2001).

³⁹S. E. Feller and A. D. MacKerell, *J. Phys. Chem. B* **104**, 7510–7515 (2000).

⁴⁰V. Vasumathi and M. N. D. S. Cordeiro, *Chem. Phys. Lett.* **600**, 79–86 (2014).

⁴¹J. Viecelli, O. L. Ma, J. Douglas, and J. D. Tobias, *J. Phys. Chem. A* **108**, 5806–5814 (2004).

⁴²Y. Dubowski, J. Viecelli, J. D. Tobias, A. Gomez, A. Lin, S. A. Nizkorodov, T. M. McIntire, and B. J. Finlayson-Pitts, *J. Phys. Chem. A* **108**, 10473–10485 (2004).

⁴³M. Szori, D. J. Tobias, and M. Roeselová, *J. Phys. Chem. B* **113**, 4161–4169 (2009).

⁴⁴H. Heinz, R. A. Vaia, B. L. Farmer, and R. R. Naik, *J. Phys. Chem. C* **112**, 17281–17290 (2008).

⁴⁵J. P. Hansen and I. R. McDonald, *Theory of Simple Liquids* (Academic Press, London, 1986).

⁴⁶S. Plimpton, *J. Comput. Phys.* **117**, 1–19 (1995).

⁴⁷R. W. Hockney, S. P. Goel, and J. W. Eastwood, *J. Comput. Phys.* **14**, 148–158 (1974).

⁴⁸S. Nose and M. L. Klein, *Mol. Phys.* **50**, 1055–1076 (1983).

⁴⁹M. Parrinello and A. Rahman, *J. Appl. Phys.* **52**, 7182–7190 (1981).

⁵⁰D. J. Hardy, J. E. Stone, and K. Schulten, *Parallel Comput.* **35**, 164–177 (2009).

⁵¹J. P. Ryckaert, G. Ciccotti, and H. J. C. Berendsen, *J. Comput. Phys.* **23**, 327–341 (1977).

⁵²W. Humphrey, A. Dalke, and K. Schulten, *J. Mol. Graphics* **14**, 33–38 (1996).

⁵³P. K. Ghorai and S. C. Glotzer, *J. Phys. Chem. C* **111**, 15857–15862 (2007).

⁵⁴A. Luzar and D. Chandler, *Phys. Rev. Lett.* **76**, 928–931 (1996).